Antibiotic susceptibility testing in less than 30 min using direct single-cell imaging

Özden Baltekin[a], Alexis Boucharin[a], Eva Tano[b], Dan I. Andersson[c], and Johan Elf[a,1]

[a]Department of Cell and Molecular Biology, Science for Life Laboratory, Uppsala University, SE-751 24 Uppsala, Sweden; [b]Department of Medical Sciences, Uppsala University, SE-751 85 Uppsala, Sweden; and [c]Department of Medical Biochemistry and Microbiology, Uppsala University, SE-751 23 Uppsala, Sweden

Edited by Nancy E. Kleckner, Harvard University, Cambridge, MA, and approved July 7, 2017 (received for review May 23, 2017)

The emergence and spread of antibiotic-resistant bacteria are aggravated by incorrect prescription and use of antibiotics. A core problem is that there is no sufficiently fast diagnostic test to guide correct antibiotic prescription at the point of care. Here, we investigate if it is possible to develop a point-of-care susceptibility test for urinary tract infection, a disease that 100 million women suffer from annually and that exhibits widespread antibiotic resistance. We capture bacterial cells directly from samples with low bacterial counts (10^4 cfu/mL) using a custom-designed microfluidic chip and monitor their individual growth rates using microscopy. By averaging the growth rate response to an antibiotic over many individual cells, we can push the detection time to the biological response time of the bacteria. We find that it is possible to detect changes in growth rate in response to each of nine antibiotics that are used to treat urinary tract infections in minutes. In a test of 49 clinical uropathogenic *Escherichia coli* (UPEC) isolates, all were correctly classified as susceptible or resistant to ciprofloxacin in less than 10 min. The total time for antibiotic susceptibility testing, from loading of sample to diagnostic readout, is less than 30 min, which allows the development of a point-of-care test that can guide correct treatment of urinary tract infection.

point of care | UTI | AST | antibiotic | resistance | microfluidic

With the ever-increasing emergence and spread of antibiotic-resistant bacteria, a key factor in correct treatment of infections is the ability to rapidly identify the antibiotic susceptibility profile of the infecting species to assure the use of an efficacious antibiotic and reduce the need for broad spectrum drugs (1–3). Phenotypic antibiotic susceptibility tests (ASTs) are typically based on the detection of differential bacterial growth with and without antibiotics in liquid cultures or on solid agar plates (4). In liquid tests, detection is based on the change in OD, whereas the disk diffusion method is used on solid agar plates to identify inhibition zones (5). These methods are generally reliable for detecting resistance and determining the antibiotic concentration that prevents bacterial growth, making them predictive of the therapeutic utility of different antibiotics. However, because it typically takes 1–2 d to get a reliable readout, these methods fail to guide treatment in the early, often critical, stages of infection. As a consequence, the physician is left with the difficult choice of prescribing a broad spectrum antibiotic or risking that the first prescribed antibiotic is ineffective.

Genotypic ASTs are based on detection of a specific genetic marker (plasmids, genes, or mutations) associated with resistance phenotypes by using the common genetic tools (e.g., sequence-specific amplification by PCR, padlock probe-mediated rolling circle amplification, or whole-genome sequencing) (3, 6). These tests are highly sensitive and can limit the detection time to what is needed to amplify selected DNA sequences to detectable levels, but they require detailed advance knowledge of which resistance markers to test for. If new resistance mechanisms arise, these would go undetected and result in false negatives. Furthermore, the presence of certain resistance genes/mutations does not necessarily translate into phenotypic resistance.

Unlike the genotypic ASTs, the phenotypic ASTs directly assess if the antibiotic stops bacterial growth, which is the most relevant measure for the treating physician. New phenotypic ASTs have, therefore, been developed in recent years to decrease the detection times. In particular, microfluidics (7) have made it possible to increase the signal to background ratio in the phenotypic assays by miniaturizing the bacterial incubation chambers (8). Using microfluidic approaches, it has been possible to push the time requirement for AST to 1–3 h (9–13). Recent promising data based on relative DNA copy number increase in antibiotic-treated vs. reference cultures quantified using digital PCR suggest that a biological response can be detected already 15 min after exposure to an antibiotic (14). However, the PCR step still takes an additional 60 min, making this test too slow for a point-of-care application. Here, we use direct single-cell imaging to show that it is possible to determine if a bacterial isolate is susceptible to an antibiotic in less than 10 min. When we include the time for loading a dilute sample, the total time for the test is less than 30 min, such as would be required for a point-of-care application.

Urinary tract infection (UTI) is one example where a fast AST could improve medical practice by making it possible to prescribe an antibiotic to which the infecting bacteria are susceptible before the patient leaves the primary care unit. A fast AST for UTI would have an important clinical impact given that there are 100 million cases of UTI per year worldwide, with high frequency of resistance to primary antibiotics (15). Because 85% of all UTI cases diagnosed in primary care are caused by *Escherichia coli*, we have focused on this species, but the test can be expanded to

Significance

Antibiotic resistance is a global threat to human health. The problem is aggravated by unnecessary and incorrect use of broad spectrum antibiotics. One way to provide correct treatment and slow down the development of antibiotic resistance is to assay the susceptibility profile of the infecting bacteria before treatment is initiated and let this information guide the choice of antibiotic. Here, we present an antibiotic susceptibility test that is sufficiently fast to be used at the point of care. We show that it is possible to determine if a urinary tract infection is caused by resistant bacteria within 30 min of loading a urine sample, even if the bacterial concentration in the urine is very low.

Author contributions: Ö.B., D.I.A., and J.E. designed research; Ö.B. performed research; E.T. contributed clinical isolates and their resistance classification; Ö.B. and A.B. analyzed data; and Ö.B., D.I.A., and J.E. wrote the paper.

Conflict of interest statement: The chip design is being patented (PCT/SE2015/050685). The fast antibiotic susceptibility test is being developed into a product by a company of which Ö.B. and J.E. are shareholders.

This article is a PNAS Direct Submission.

Freely available online through the PNAS open access option.

[1]To whom correspondence should be addressed. Email: johan.elf@icm.uu.se.

This article contains supporting information online at www.pnas.org/lookup/suppl/doi:10.1073/pnas.1708558114/-/DCSupplemental.

also include other species. Clinical infections are diagnosed from 10^3 or 10^4 cfu/mL depending on country, which defines the required sensitivity of a test.

Results

Design and Loading of Microfluidic Chip. The microfluidic chip design is shown in Fig. 1. (More details on the design can be found in *SI Materials and Methods* and Figs. S1 and S2.) The device has two rows of cell traps. In each row, there are 2,000 cell traps of dimension 1.25 × 1.25 × 50 μm (Fig. 1*A*) that can be loaded with bacterial cells (red) from the front channel. A constriction at the end of each trap prevents cells from passing to the back channel, while allowing the media to flow around the cells. This sieve-like design, which is an extension of the Mother Machine (16), enables rapid loading and constant media flow over the cells.

To test how rapidly dilute samples could be loaded, we monitored the fraction of traps loaded over time for different cell cultures with densities from 1,100 to 2×10^6 cfu/mL (Fig. 1*B*); 80% of the cell traps were filled within 30 s at a cell density of 2×10^6, and even with the most dilute sample, 1,100 cells per 1 mL, 160 of 2,000 traps were filled in 10 min (*SI Materials and Methods* and Fig. S3).

The loading time curves (Fig. 1*B*) can be used for real time bacterial density determination (for example, in a urine sample). Within 30 s, it would be possible to assess if it was a severe bacterial infection with more than 10^5 cells per 1 mL, and within 10 min, it would be possible to determine if there is a clinically relevant infection at all (17, 18).

Growth Rate Measurements. In a typical experiment, fluid control is switched from loading to running mode when there is at least one cell in one-half of the cell traps. This prevents filling the cell traps and allows easy detection of the front end of the cell column. A few seconds after the switch, loading media inflow stops, and test media start to reach the cell trap regions. The reference population row receives the antibiotic-free medium, and the treatment population row receives the media with the antibiotic to be tested (Fig. 2*A*). After the media switch, we performed time-lapse phase contrast microscopy (20× magnification) with an automated *x*–*y* translation stage, where each of 4,000 cell traps was imaged every 60 s (a time-lapse movie of one position during a typical experiment can be seen in Movie S1).

Growth rates were first estimated for the cells in each individual cell trap. The movement of the front-most cell pole in each cell trap was monitored as a proxy for the cumulative cell length changes for the cells within that trap. Fig. 2 *B*–*D* shows an example of how the average growth rate for the cells in an individual cell trap was calculated for the reference cells without antibiotics (Fig. 2 *B*, *Left*; *C*, *Left*; and *D*, *Left*) and antibiotic-treated cells (Fig. 2 *B*, *Right*; *C*, *Right*; and *D*, *Right*). Fig. 2*B* shows one cell trap every fifth frame of a 120-frame (60-min) experiment, and the circles (blue or red) show the detected front-most cell pole position at that frame. In Fig. 2*C*, the solid dots (blue or red) show the length of the cell(s) within that cell trap through the experiment. Fig. 2*D* shows the instantaneous growth rate estimated as the relative length increase per time in a sliding window over 10 min.

Distinguishing Two Populations Based on Growth Rate Statistics. In Fig. 2 *E*–*H*, we applied the growth rate calculation for each of 2,000 cell traps in both rows, such that Fig. 2*E* shows length vs. time for the two populations (the reference population is in Fig. 2*E*, *Left*, and the treatment population is in Fig. 2*E*, *Right*). The

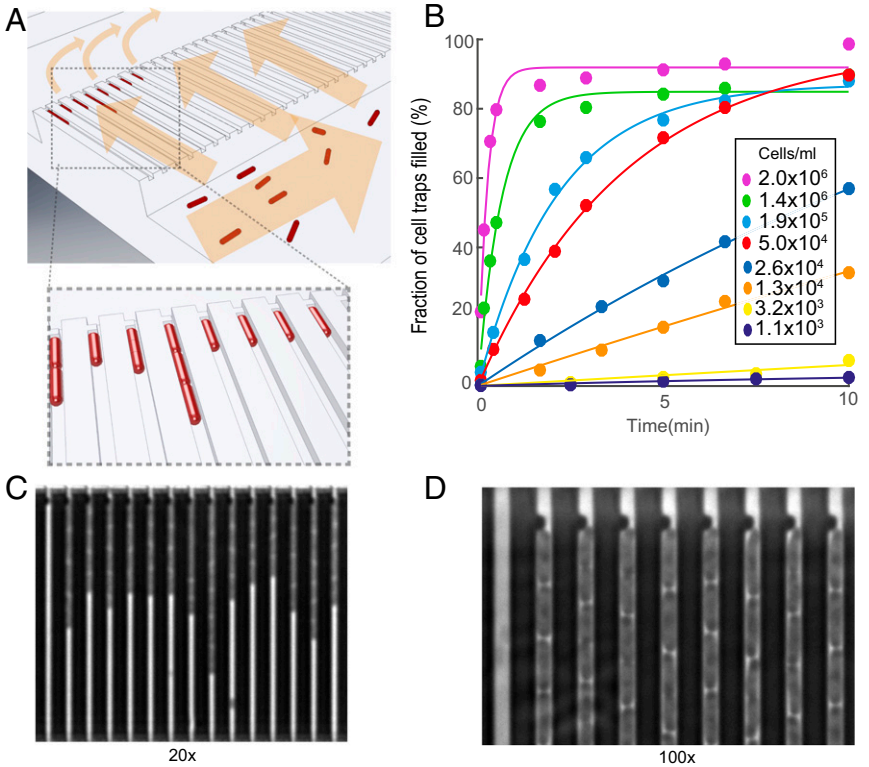

Fig. 1. Design and operation details of the microfluidic chip. (*A*) Cartoon illustrating the loading of rod-shaped bacterial cells (red) into cell traps. Arrows indicate flow direction during loading. (*B*) Fraction of cell traps with at least one *E. coli* cell at different time points. The different markers correspond to different density cell cultures. (*C*) A phase contrast image of *E. coli* in the microfluidic device (darker regions) using a 20× objective. (*D*) A small part of a phase contrast image taken at 100× showing the back end of the cell trap, where the flow restriction region captures the cells during loading.

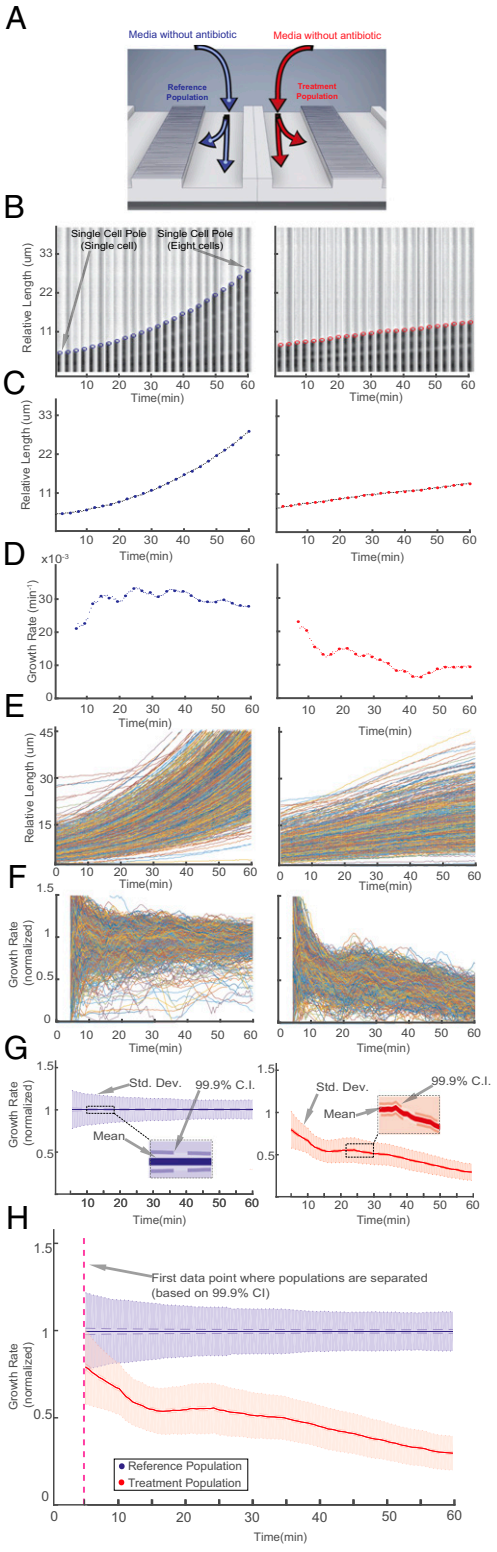

Fig. 2. Detection of growth rate effect of antibiotic. (*A*) Media with or without antibiotic are supplied to the two different rows of cell traps to test the effect of the antibiotic (CIP; 1 μg/mL) on the treatment population compared with the reference population. (*B*) A single-cell trap from the reference population (*Left*) and another single-cell trap from the treatment population (*Right*) are shown every fifth frame (every 2.5 min). The detected front-most cell pole position is given as a blue or red circle. (*C*) The corresponding length change through time is shown with the blue or red dots. (*D*) Growth rates calculated with a sliding window of up to 10 min (starting at 5 min). The (*E*) length and (*F*) growth rate are plotted as a function of time for all of the individual traps for the reference (*Left*) and the treatment population (*Right*). (*G*) The descriptive statistics of the normalized growth rate distributions for these populations are shown as a function of time. Colored as blue for the reference population (*Left*) and red for antibiotic treated population (*Right*), solid lines show the mean, dark-shaded regions show the 99.9% confidence interval (99.9% CI) of the mean, and the light-shaded region shows the sample SDs. (*H*) The overlay of the two population's normalized growth rate distributions. The time of separation of the treatment population from the reference population based on 99.9% CIs occurs before the dashed magenta line, which indicates the first time point when growth rates are estimated.

corresponding growth rates for individual traps are shown in Fig. 2*F*. In Fig. 2*G*, the growth rates for the individual cell traps from both populations are averaged and normalized by the average growth rate of the reference population. The framewise sample SD is shown in light transparent color in Fig. 2*G*, and the SEM is used to calculate a 99.9% confidence interval for the average growth rate (darker shaded region in Fig. 2*G*). By combining the data from the two columns (Fig. 2*H*), we could detect the response of the antibiotic treatment population in this experiment based on divergence from a 99.9% confidence interval (dashed magenta line in Fig. 2*H*) earlier than the first data point at ∼5 min.

Fast Detection of Response to Antibiotic Treatment. Using the fast antibiotic susceptibility test (fASTest), we determined the antibiotic response time of *E. coli* (MG1655) to nine different antibiotics that are used for UTIs. These included three different types of penicillins [ampicillin (AMP), amoxicillin-clavulanate (AMX-CLA), and mecillinam (MEC)], one carbapenem [doripenem (DOR)], two different fluoroquinolones [ciprofloxacin (CIP) and levofloxacin (LEV)], and three other agents [fosfomycin (FOS), nitrofurantoin (NIT), and trimethoprim-sulfamethoxazole (TMP-SMX)]. We followed The European Committee on Antimicrobial Susceptibility Testing (EUCAST) breakpoint value recommendations for the test concentrations of each particular antibiotic and the testing media requirements. We loaded the bacteria into the microfluidic chip and supplied growth media (GM) without antibiotic to one row (reference population) and GM with antibiotic to the other (treatment population). With this setup, we could detect the differential growth rate between treatment and reference populations in 3 min for CIP, LEV, MEC, NIT, and TMP-SMX; 7 min for AMX-CLA and DOR; 9 min for FOS; and 11 min for ampicillin based on 99.9% confidence intervals (Fig. 3).

Importantly, the response curves were very reproducible between biological replicates, as shown for CIP and ampicillin in *SI Materials and Methods* and Fig. S4. This implies that the differential responses to the different drugs were not caused by limited time resolution in the assay but rather, that the measurement was sufficiently fast to monitor the actual biological response time. These experiments were run in the standard susceptibility testing Mueller–Hinton (MH) media; however, in *SI Materials and Methods*, we show that response times were similar for bacteria grown in urine (Fig. S5). In *SI Materials and Methods* and Movies S2 and S3, we also show that the fASTest works on *Klebsiella pneumoniae* and *Staphylococcus saprophyticus*, which are two other major pathogens causing uncomplicated UTI. The response time for *S. saprophyticus* was slower as expected because of its longer generation time (Fig. S6).

Fast Antibiotic Susceptibility Testing of Clinical Isolates. To be practically useful, fASTest needs to differentiate between strains with clinically relevant spectra of resistance mutations and susceptible strains in their responses to the antibiotic. This is important, because even resistant bacteria can show a growth rate reduction caused by the presence of an antibiotic, and one cannot, therefore,

MICROBIOLOGY

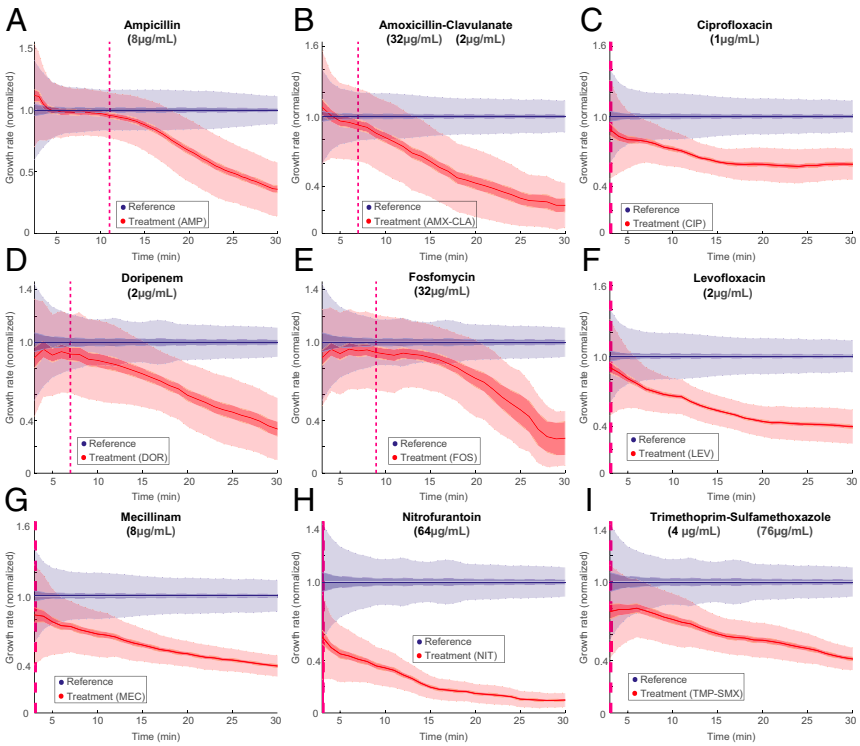

Fig. 3. Fast detection of response to antibiotic treatment. fASTest experiments testing how fast susceptible *E. coli* cells respond to (*A*) ampicillin, (*B*) AMX-CLA, (*C*) CIP, (*D*) DOR, (*E*) FOS, (*F*) LEV, (*G*) MEC, (*H*) NIT, and (*I*) TMP-SMX. AMP, ampicillin.

directly conclude that a strain is susceptible just because it has impaired growth compared with untreated cells (as seen in Fig. 3). For this reason, we first tested CIP susceptibility of an *E. coli* strain that was genetically engineered to be resistant to ciprofloxacin (CipR) because of the introduction of several clinically observed mutations (*gyrA1*-S83L *gyrA2*-D87N *parC*-S80I) (19) and compared the results with those of the congenic susceptible WT *E. coli* strain (CipS) (Fig. 4 *A* and *B*). During the first minutes of the test, the CipR strain grew slightly slower when treated with CIP than its untreated reference population (Fig. 4*A*) before recovering to the same growth rate. The CipS strain responded more strongly (Fig. 4*B*), which made it possible to distinguish the WT strain from its constructed resistant counterpart in a few minutes.

Next, we tested 50 clinical isolates of uropathogenic *E. coli* (UPEC) strains for CIP susceptibility. Samples were initially collected and characterized by the Uppsala University Hospital Clinical Microbiology Laboratory using the gold standard disk diffusion test for CIP susceptibility/resistance as a part of routine for clinical diagnosis. The antibiotic susceptibility of isolates was tested by the disk diffusion method recommended by the European Committee on Antimicrobial Susceptibility Testing (5). A total of 25 CIP-susceptible and 25 CipR isolates were given to us. We received those samples blinded: without the patient or the CIP susceptibility information. One isolate did not grow in the liquid cultures during the preparations and was, therefore, excluded from the study. The remaining 49 isolates were tested for CIP susceptibility using the fASTest. Subsequently, the results were compared with the results from the hospital.

The fASTest results of 49 UPEC clinical isolates are given in Fig. 4 *C*–*E*. The growth rate of the untreated reference population varied between the isolates without any obvious differences between resistant and susceptible isolates (Fig. 4*C*). CIP growth rates of treated populations did not reveal a striking distinction between the resistant and the susceptible isolates (Fig. 4*D*). However, when the growth rate of the CIP-treated population was normalized with the growth rate of the untreated reference population from the same experiment, susceptible and reference isolates grouped apart after the first 10 min (Fig. 4*E*). As can be seen in Fig. 4*E*, all of 24 resistant strains and 25 susceptible strains were grouped in agreement with gold standard disk diffusion measurements within 10 min. This complete agreement corresponds to 86.28–100.00% sensitivity and 85.75–100.00% specificity for detecting resistance.

Discussion

This study originated in an investigation of the cell to cell variation in the bacterial cell cycle (20), which required us to develop tools to determine growth rates very accurately for individual *E. coli* cells. The process of averaging the growth rate from several hundred individual bacteria makes it possible to detect changes in growth as fast as the biological responses to the antibiotic (Fig. S4). For this reason, it is not possible to find a phenotypic AST based on the growth rate response that is faster than the fASTest. It is important to note that the same time resolution cannot be achieved in a bulk measurement of the growth rate, because in that case, the averaging is done over the cells before the readout, which means that the unavoidable readout noise will impact the growth rate estimate much more than if it is averaged over the cells after the readout.

The sensitivity of fASTest in terms of how many cells per milliliter can be detected is only dependent on how much time is spent loading the cells. For 10^4 cfu/mL, which is in the lower range for clinically relevant UTIs, sufficient loading can be achieved in 5 min, because for fASTest, it is sufficient to collect ≈100 bacteria. However, the sensitivity will practically depend on which body fluid the sample is collected from. For example, in UTI samples, there may be bacterial contamination from the skin or vaginal flora that sets the sensitivity limit for the infecting species. However, cell traps that contain contaminants may in many cases be excluded based on the morphology and growth rate of the contaminants.

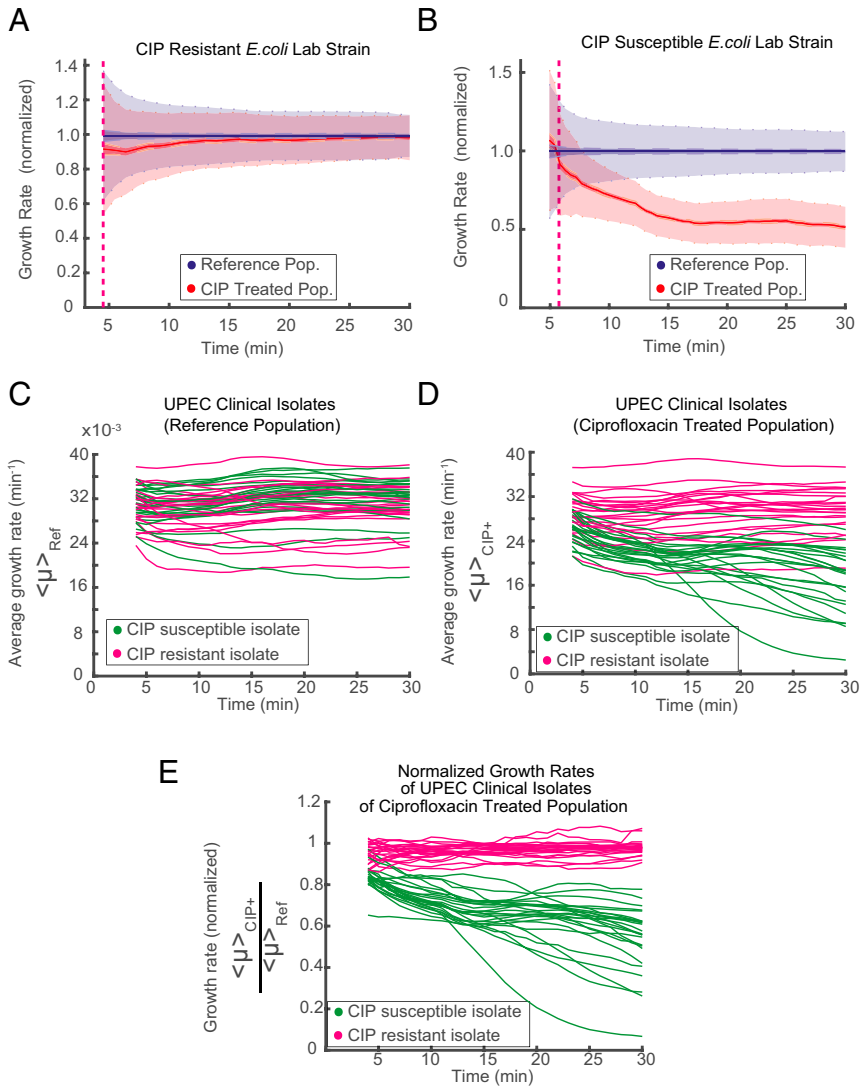

Fig. 4. fASTest for resistant and susceptible strains. Laboratory strains of (*A*) CIP-resistant and (*B*) -susceptible *E. coli* are tested for CIP susceptibility. (*C–E*) Forty-nine clinical isolates of UPEC are tested with fASTest for CIP susceptibility. (*C*) Average growth rates for the reference populations. (*D*) Average growth rates for the treatment populations. Color coding indicates magenta for clinically resistant to CIP and green for clinically susceptible to CIP. (*E*) Growth rate of treated populations normalized for the growth rate of the respective reference population.

A challenge related to contamination is polymicrobial infections. These are rare for uncomplicated UTIs but commonly observed for, for example, catheter users (21). Because we detect all bacteria in the sample and do not only detect those that grow under standard plating assays, polymicrobial infections can be detected as a high diversity of growth rates in the reference channel. If the mixed strains also display a diverse resistance pattern, this would be observed as a broadened growth rate distribution after antibiotic treatment. An actual point-of-care test would, therefore, have to consider other aspects of the growth rate distribution than just the average. There may, for example, be specific automated indications if a few individual bacteria keep growing fast in a background of dying cells, because this may indicate a polymicrobial infection with a complex resistance spectrum. An alternative strategy for the test to deal with polymicrobial infections and contaminations is to make it time sequential, such that the growth rate is determined for the cells in each cell trap before and after antibiotic treatment. This allows for focusing the analysis on only growing cells and avoiding biases in the averaging caused by an uneven distribution of different species between the reference channel and the treatment channel. A test also needs to consider the possible situation where the cells in the reference channel grow so slowly that a lack of response in treatment channel would be unreliable.

We have here focused on bacterial species and antibiotics related to UTIs, but it is likely that the same principles would work for sepsis, mastitis, or meningitis (i.e., in blood, milk, or cerebrospinal fluid that normally should be devoid of bacterial-sized cells). Independent of the sample, the key principle will be true: it is sufficient to measure the single-cell growth of a few hundred bacteria to get very close to the theoretical time limit for monitoring the response to an antibiotic in real time.

In summary, samples with more than 10^4 cfu/mL can be loaded in less than 10 min, and thus, no precultivation is needed for patient urine samples. Furthermore, any eukaryotic cell in the sample will be too large to pass through the filtration region within the microfluidic chip or enter the cell channels and disturb the assay. Thus, the combined AST time (loading, measurement, and readout) of the sample is less than 30 min. Based on the small clinical study of CIP susceptibility, the observed sensitivity and specificity of the

assay are in 100% agreement with existing but prohibitively slow methodology.

Materials and Methods

The Microfluidic Chip. The microfluidic chip consists of a cover glass (1.5) and a micromolded silicon elastomer [Sylgard 184; polydimethylsiloxane (PDMS)] that are covalently bonded together. For micromolding, we used the standard soft lithography techniques as described in *SI Materials and Methods*.

fASTest Protocol. All of the fASTest runs described in this paper follow this common protocol: growth of overnight culture (ONC), growth of loading culture, connection of microfluidic flow control setup to the microfluidic chip, aligning the chip to the camera, selection of positions to be imaged, running an imaging test to ensure the stability of the microfluidic chip, connecting the loading culture to the macrofluidic setup, loading the cells from loading culture, and starting the antibiotic application and automated phase contrast microscopy.

Bacterial Strains. The strains used were WT strain DA5438 (*E. coli* MG1655), ampicillin-resistant strain DA28097 [*E. coli* del(P*lacI_lacIZYA*)::amp], CipR strain DA20859 (*E. coli gyrA1*-S83L, *gyrA2*-D87N, parC-S80I), and two other species: DA12755 (*K. pneumoniae*; ATCC13883) and DA14015 (*S. saprophyticus*).

GM. Depending on the experiment, we used either Mueller–Hinton Broth (70192–500G; Sigma-Aldrich) or urine as GM. When indicated, the GM was supplemented with an antibiotic. In preparation of urine media, morning urine was collected, and filtered (nitrocellulose filter; 0.2-μm pore size). All media are supplemented with a surfactant [Pluronic F-108; 542342; Sigma-Aldrich; 0.085% (wt/vol) final concentration] to prevent the attachment of the bacteria to the PDMS surface.

Culture Conditions. For ONC, bacteria from the glycerol stocks were inoculated into 2 mL GM and incubated (37 °C; shaking at 225 rpm) for ∼16 h. For loading culture, 2.5 μL ONC is diluted 1:800 to a total of 2 mL GM and incubated (37 °C; shaking at 225 rpm) for 120 min. For growth in the chip, the chip was continuously supplied with GM and incubated in the microscope cage incubator at 37 °C before, during, and after the loading of bacterial culture and also, during the test. The loading culture was connected to the fluidic setup and kept in the cage incubator at 37 °C. GM was kept outside of the cage incubator at room temperature (21 °C).

Microfluidic Flow Control Setup Details. Flow direction and rate during the experiment were maintained by pressure-driven flow. An electropneumatic controller from Elveflow (OB1 MkIII) regulated the air pressure applied to the closed fluidic reservoirs. Pressures, flow rates, and tubing details are explained in *SI Materials and Methods*. The electropneumatic controller was programmed in MATLAB.

Automated Phase Contrast Microscopy. We used a Nikon Ti-E inverted microscope with a 20× objective (CFI Plan Apo Lambda DM 20× or CFI S Plan Fluor ELWD ADM 20×), with a motorized *x–y* stage, and a CMOS camera (DMK23U274; The Imaging Source). The setup was maintained within the Cage Incubator Enclosure (custom made by Okolab), where the temperature was maintained at 37 °C by a temperature controller (Airtherm-Atx; World Precision Instruments). Both the microscope and the camera were controlled by an open source microscopy software (MicroManager 1.4.19). Phase contrast images were acquired by the software's multidimensional acquisition feature, through which the motorized stage moved the fluidic chip to 36 different positions. Each position was imaged every 30 or 60 s depending on the particular experiment. Each experiment was 30 min, although the imaging could be continued longer if needed to provide insights on kill dynamics.

Image Processing. The images were processed for detection of each row in the raw image and cell traps and empty traps in each row, removing background and performing pole detection to obtain the cell pole detection in each frame of each position using an algorithm developed in MATLAB. Details of this algorithm are given in *SI Materials and Methods* and Fig. S7.

Data Analysis. For cell pole tracking, we used μTrack (22). For growth rate calculation of individual cells, we applied a sliding window of data points (length) and fitted a linear function to the logarithm of them. The sliding window grows from 2 to 10 min in the beginning of the experiment and stays at 10 min afterward. We filtered some data based on fixed criteria to remove misidentified particles or cells that were dead from the beginning as well as the traps that were overly filled or left empty during the loading. Details of filters applied are given in *SI Materials and Methods*.

All raw data will be made available upon request for noncommercial interests. The ethical review committee in Uppsala has no objection to this study (reference no. 2017/051).

ACKNOWLEDGMENTS. This work was supported by the Swedish Research Council (D.I.A. and J.E.), the European Research Council (J.E.), and the Knut and Alice Wallenberg Foundation (J.E.).

1. Kerremans JJ, et al. (2008) Rapid identification and antimicrobial susceptibility testing reduce antibiotic use and accelerate pathogen-directed antibiotic use. *J Antimicrob Chemother* 61:428–435.
2. Doern GV, Scott DR, Rashad AL (1982) Clinical impact of rapid antimicrobial susceptibility testing of blood culture isolates. *Antimicrob Agents Chemother* 21:1023–1024.
3. van Belkum A, et al. (2013) Rapid clinical bacteriology and its future impact. *Ann Lab Med* 33:14–27.
4. Jenkins SG, Schuetz AN (2012) Current concepts in laboratory testing to guide antimicrobial therapy. *Mayo Clin Proc* 87:290–308.
5. Matuschek E, Brown DFJ, Kahlmeter G (2014) Development of the EUCAST disk diffusion antimicrobial susceptibility testing method and its implementation in routine microbiology laboratories. *Clin Microbiol Infect* 20:O255–O266.
6. Frickmann H, Masanta WO, Zautner AE (2014) Emerging rapid resistance testing methods for clinical microbiology laboratories and their potential impact on patient management. *BioMed Res Int* 2014:375681.
7. Reece A, et al. (2016) Microfluidic techniques for high throughput single cell analysis. *Curr Opin Biotechnol* 40:90–96.
8. Murray C, Adeyiga O, Owsley K, Di Carlo D (2015) Research highlights: Microfluidic analysis of antimicrobial susceptibility. *Lab Chip* 15:1226–1229.
9. Kim SC, Cestellos-Blanco S, Inoue K, Zare RN (2015) Miniaturized antimicrobial susceptibility test by combining concentration gradient generation and rapid cell culturing. *Antibiotics (Basel)* 4:455–466.
10. Choi J, et al. (2013) Rapid antibiotic susceptibility testing by tracking single cell growth in a microfluidic agarose channel system. *Lab Chip* 13:280–287.
11. Hou Z, et al. (2014) Time lapse investigation of antibiotic susceptibility using a microfluidic linear gradient 3D culture device. *Lab Chip* 14:3409–3418.
12. Choi J, et al. (2014) A rapid antimicrobial susceptibility test based on single-cell morphological analysis. *Sci Transl Med* 6:267ra174.
13. Quach DT, Sakoulas G, Nizet V, Pogliano J, Pogliano K (2016) Bacterial cytological profiling (BCP) as a rapid and accurate antimicrobial susceptibility testing method for Staphylococcus aureus. *EBioMedicine* 4:95–103.
14. Schoepp NG, et al. (2016) Digital quantification of DNA replication and chromosome segregation enables determination of antimicrobial susceptibility after only 15 minutes of antibiotic exposure. *Angew Chem Int Ed Engl* 55:9557–9561.
15. Stamm WE, Norrby SR (2001) Urinary tract infections: Disease panorama and challenges. *J Infect Dis* 183:S1–S4.
16. Wang P, et al. (2010) Robust growth of Escherichia coli. *Curr Biol* 20:1099–1103.
17. Slekovec C, et al. (2012) Impact of a region wide antimicrobial stewardship guideline on urinary tract infection prescription patterns. *Int J Clin Pharm* 34:325–329.
18. Schmiemann G, Kniehl E, Gebhardt K, Matejczyk MM, Hummers-Pradier E (2010) The diagnosis of urinary tract infection: A systematic review. *Dtsch Arztebl Int* 107: 361–367.
19. Marcusson LL, Frimodt-Møller N, Hughes D (2009) Interplay in the selection of fluoroquinolone resistance and bacterial fitness. *PLoS Pathog* 5:e1000541.
20. Wallden M, Fange D, Lundius EG, Baltekin Ö, Elf J (2016) The synchronization of replication and division cycles in individual E. coli cells. *Cell* 166:729–739.
21. Kline KA, Lewis AL (2016) Gram-positive Uropathogens, polymicrobial urinary tract infection, and the emerging microbiota of the urinary tract. *Microbial Spectr*, 10.1128/microbiolspec.UTI-0012-2012.
22. Jaqaman K, et al. (2008) Robust single-particle tracking in live-cell time-lapse sequences. *Nat Methods* 5:695–702.
23. Loy G, Zelinsky A (2003) Fast radial symmetry for detecting points of interest. *IEEE Trans Pattern Anal Mach Intell* 25:959–973.
24. Seber GAF, Lee AJ (2003) Linear regression: Estimation and distribution theory. *Linear Regression Analysis* (Wiley, Hoboken, NJ), 2nd Ed. pp 35–95.